Atomic Force Microscope Measurements of Nucleosome Cores Assembled along Defined DNA Sequences†

Michael J. Allen,*,‡ X. Fan Dong,‡ Timothy E. O'Neill,‡,§ Peter Yau,‡ Stephen C. Kowalczykowski,∥ Joe Gatewood,⊥ Rod Balhorn,# and E. Morton Bradbury‡,⊥

Departments of Biological Chemistry, School of Medicine, and Microbiology, University of California, Davis, California 95616, Life Sciences Division, Los Alamos National Laboratory, Los Alamos, New Mexico 87545, and Biology and Biotechnology Research Program, Lawrence Livermore National Laboratory, Livermore, California 94550

Received April 23, 1993; Revised Manuscript Received June 9, 1993

ABSTRACT: We have found that the atomic force microscope (AFM) can be used to image the "beads-on-a-string" chromatin structure in a normal air environment following adsorption onto a cover glass substrate. Individual nucleosome cores and linker DNA could be resolved clearly along chromatin fibers that were reconstituted using histone octamers and a tandemly repeated 208-bp nucleosome positioning DNA sequence (208–18). AFM measurements showed that the compaction of the 3780-bp DNA by different loadings of histone octamers was consistent with 146 bp of DNA wrapped 1.75 turns about the histone octamer to form the 11-nm nucleosome core. Precise internucleosome core spacing measurements could be performed along the chromatin fiber axis. In other experiments, AFM images of chromatin reconstituted using closed circular DNA showed highly tangled beaded fibers, as expected. These images and measurements demonstrate that AFM can provide useful high-resolution structural information about chromatin that can be used to complement other more established techniques such as electron microscopy.

The atomic force microscope (AFM) is relatively new (Binnig et al., 1986), and a number of different biological samples have been imaged (Allen et al., 1992; Butt et al., 1990; Haberle et al., 1991; Hansma et al., 1992b; Henderson et al., 1992; Singh & Keller, 1991; Wiegrabe et al., 1991) including native chromatin (Vesenka et al., 1993b) and metaphase chromosomes (De Grooth & Putman, 1992). Successful imaging of biological structures with the AFM represents a clear improvement, in some cases, over the limitations of the scanning tunneling microscope, which requires sometimes destructive tunneling currents and the use of conductive specimens and supports. The AFM design used in the present study utilizes a sharpened contact probe, mounted on a flexible cantilever, that is scanned gently and precisely across the sample surface. The vertical displacements of the AFM probe (≥0.02 nm) are detected using a photodiode aligned with a laser beam that is reflected off the back of the probe. A detailed description of AFM and the principles behind its operations have been presented in several articles and reviews (Engel, 1991; Hansma et al., 1988; Heinzelmann et al., 1990; Hoh & Hansma, 1992). The AFM images hydrated biological structures using simple, rapid sample preparations without the need for strains or metal coatings. Resolutions attained closely approach and in some cases exceed those of the electron microscope (EM). For example, the application of the AFM to measure sample thicknesses in air and fluid environments has already proved to be particularly useful in studies of chromatin compaction within the sperm nucleus (Allen et al., 1991; Da Silva et al., 1993). Several laboratories have reported recently that DNA molecules deposited on the surface of mica can be imaged reproducibly by AFM (Bustamante et al., 1992; Hansma et al., 1993; Lyubchenko et al., 1993b; Vesenka et al., 1992a). Routine imaging of DNA is a major advance toward useful biological applications of the AFM. However, other advances that are still needed include (1) the development of new AFM substrates, in addition to mica, for biological work and (2) the observation of high-resolution AFM images of a number of important protein–DNA complexes. In our laboratory, we are currently investigating higher order chromatin structures. Recently, we have found that reproducible high-resolution AFM images of reconstituted chromatin fibers can be achieved using cover glass as the AFM substrate. Because the precise length of the DNA molecule used in our study is known, using AFM, we can measure the compaction ratios of the DNA for a range of loadings of nucleosome cores formed by histone octamers. Also, we were able to determine precisely the spacings of the nucleosome cores along the chromatin fiber axis from the AFM images.

We report the first AFM images of chromatin fibers (reconstituted using defined DNA sequences) that provide useful high-resolution information about DNA packaging within the nucleosome. In addition, these images demonstrate the ability of AFM to complement other established methods, such as EM. The apparent dimensions of the nucleosome cores and linker DNA in AFM images and the sharpness of the AFM probe are discussed.

MATERIALS AND METHODS

Chromatin Samples Reconstituted Using Linear DNA. A 3.78-kbp linear DNA fragment containing 18 tandem repeats of the 208-bp nucleosome positioning sequence of the *Lytechinus variegatus* 5S rRNA gene (208–18) was isolated

† This work is supported by grants from DOE (DEFG0388ER60673) and NIH (GM-26901) to E.M.B., from NIH (AI-18987) to S.C.K., and from DOE (W-7405-ENG-48) to R.B.

* To whom correspondence should be addressed: 916-752-3314 (phone); 916-752-3516 (FAX).

‡ Department of Biological Chemistry, University of California.

§ Current address: Laboratory of Molecular Embryology, National Institute of Child Health and Human Development, Bldg 6, Rm B1A13, NIH, Bethesda, MD 20892.

∥ Department of Microbiology, University of California.

⊥ Los Alamos National Laboratory.

Lawrence Livermore National Laboratory.

0006-2960/93/0432-8390$04.00/0

as described previously (Simpson et al., 1985). Chicken histone octamers were reconstituted onto linear DNA fragments by salt gradient dialysis as described previously (Norton et al., 1989). Following reconstitution using a range of different histone octamer/DNA ratios, linear chromatin fibers were fixed by dialysis against 5 mM TEA-HCl (pH 7.0), 10 mM NaCl, 0.2 mM EDTA, and 0.1% glutaraldehyde and then spread on the cover glass.

Chromatin Samples Reconstituted Using Closed Circular DNA and Cross-Linked Histone Octamers. Histone octamers were prepared from HeLa nuclei as described previously (Norton et al., 1989). Extensively cross-linked histone octamers were prepared by treatment of nucleosome cores with dimethyl suberimidate as described previously (Stein et al., 1977; O'Neill et al., 1993). Control or extensively cross-linked histone octamers were reconstituted onto closed circular pT207–18 DNA by a modification of the salt dilution method of Germond et al. (1976), as described previously (O'Neill et al., 1992, 1993). pT207–18 also contains the 3.78-kbp nucleosome positioning array described above. The closed circular chromatin was dissolved in 20 mM HEPES (pH 7.5), 50 mM NaCl, 0.5 mM EDTA, and 0.1 mM PMSF before being spread on the cover glass.

AFM Imaging of Linear and Circular Chromatin. The linear chromatin fibers were adsorbed from solution by incubating an 8-μL droplet of 1–10 μg/mL chromatin that was gently spread onto the cover glass for 10 min at room temperature. The sample preparation for the circular chromatin was the same except that the concentration was increased to 15 μg/mL and incubation time on the cover glass was 2 min. The cover glass was then rinsed briefly with a gentle flow of distilled/deionized water to remove any excess unbound material, wicked dry, and immediately scanned at room humidity (45 ± 5%) using the Nanoscope III AFM (Digital Instruments, Santa Barbara, CA). All of the images were obtained using the static, repulsive mode at a constant force minimized to just above probe pulloff. We observe very little probe adhesion on the cover glass provided fresh, maximally sharp probes are used. Slower scanning frequencies such as 5 Hz for a 5-μm^2 area were used for collecting 512 × 512 data points in all images presented. All images are unfiltered, raw data other than for occasional corrections or "flattening" of background sloping. Both etched Si nanoprobes (provided by Digital Instruments, Santa Barbara, CA) and electron beam deposited carbonized probes grown off the ends of Si_3N_4 AFM probes were used for imaging. Repeated scans of the chromatin fibers did not dislodge or appear to damage the fibers.

RESULTS

Cover Glass as an AFM Substrate. We have found that fresh cover glass (Corning, No. 1) is a highly suitable substrate for AFM since it exhibits a remarkably flat surface structure with typical local mean roughnesses of only 1.5 Å over a 500-nm^2 area. For comparison, the surface roughness of mica over 500 nm^2 is approximately 1 Å. Untreated, "out of the box" cover glass surfaces are hydrophobic, causing the chromating droplets to bead slightly on the glass. In contrast to the extensive pretreatments described for imaging DNA on mica (Vesenka et al., 1992a), the chromatin fibers will readily bind to the cover glass from solution without the need for any particular pretreatment of the glass. However, although locally flat, over larger scans untreated cover glass may exhibit a number of raised areas or bumps. Although it is not necessary for obtaining images of the chromatin fibers, these bumps can be removed by briefly rinsing the cover glass surface with either distilled water or 95% ethanol.

AFM Images of Linear 208–18 Chromatin Fibers. Figure 1 shows lower resolution linear 208–18 chromatin fibers that were adsorbed from solution onto the cover glass and immediately imaged with the AFM. These preparations typically resulted in homogeneous spreading of the chromatin fibers onto the cover glass with densities of 1–10 fibers/μm^2. Similar to reports by Shaiu et al. (1993) on AFM images of DNA molecules tagged with gold spheres, in many of our AFM images some of the chromatin fibers were aligned in the same direction on the cover glass (Figure 1A,B). Possibly local flow properties of the surrounding fluid during the adsorbing and/or rinsing steps cause the alignment. Although the level of resolution of the nucleosome cores and linker DNA along a single chromatin fiber varies depending on the sharpness of the particular AFM probe used, lower resolution images of the chromatin fibers (similar to those shown in Figure 1) are obtained routinely using the cover glass as the AFM substrate.

AFM Measurements of Compaction of the 208–18 DNA Sequence by Histone Octamers. Thus far we have been able to make AFM measurements on 14 linear chromatin fibers that were resolved clearly enough for end-to-end contour length measurement and nucleosome core scoring (Figure 2). Many of the other linear fibers imaged were not well extended, and their contour lengths could not be determined accurately. Occasionally, individual cores along a particular fiber were not easily distinguishable (likely due to a dull imaging probe), and core scoring could not be performed.

The AFM results (Figure 3) show that, with increasing loading of histone octamers on the 208–18 DNA sequence, the lengths of the chromatin fibers decreased at an incremental rate consistent with 146 bp of DNA packaged into nucleosome cores. The expected compaction values (solid line) plotted for the 3.78-kbp DNA sequence packaged by 146-bp nucleosome cores follow the linear equation $(y) = -38.64(x) + 1285.2$. Most of the AFM measurements were reasonably close to the expected values. However, some of the chromatin fiber length measurements by the AFM give compaction ratios that suggest that some of the nucleosome cores for that particular fiber contained slightly more or less than 146 bp of DNA (e.g., the chromatin fibers with 7 and 14 nucleosome cores along their lengths must contain cores with less than 146 bp of DNA). The points that gave the closest fit to the above equation (those with standard error bars) were obtained from measurements of several chromatin fibers containing the same number of nucleosome cores. Figure 2B displays an AFM image of a 208–18 chromatin fiber in which 12 of the 18 nucleosome-locating positions are filled by nucleosome cores. The remaining 6 unfilled positions can be identified by their spacings along the chromatin fiber (see arrows). However, precise positioning of the cores on the 208–18 DNA sequence was not as apparent in other images (e.g., Figure 2C). At least for the chromatin fibers imaged by AFM (which is $\ll$1% of the chromatin fibers originally incubated on the cover glass), it appears that precise positioning of the cores along the 208–18 DNA sequence is not followed strictly.

AFM Measurements of Nucleosome Spacings along the 208–18 DNA Sequence. For a sharp AFM imaging probe with a fairly uniform, rounded end, center-to-center measurements between adjacent nucleosome cores along the chromatin fiber axis are not affected by probe–sample shape convolutions. For those cores directly adjacent along a chromatin fiber (i.e., positioned such that they appear nearly

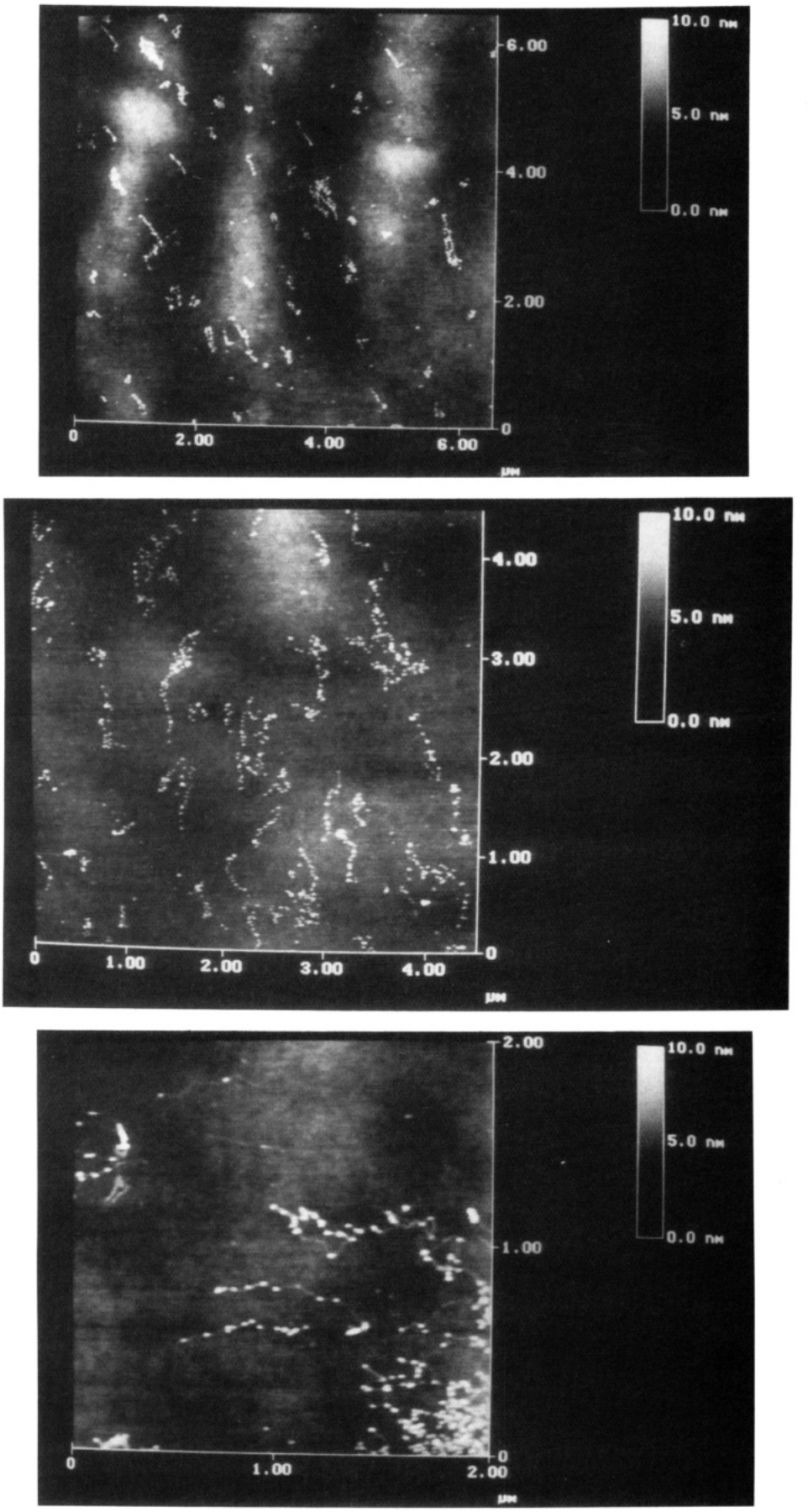

FIGURE 1: (A–C, top to bottom) Lower resolution AFM images of numerous linear 208–18 chromatin fibers (some are clumped or tangled and others straight) adsorbed from solution onto cover glass. The beaded nucleosome structures are visible in all of the images, especially along the isolated straight fibers in (B) and (C). Images were obtained using etched Si probes.

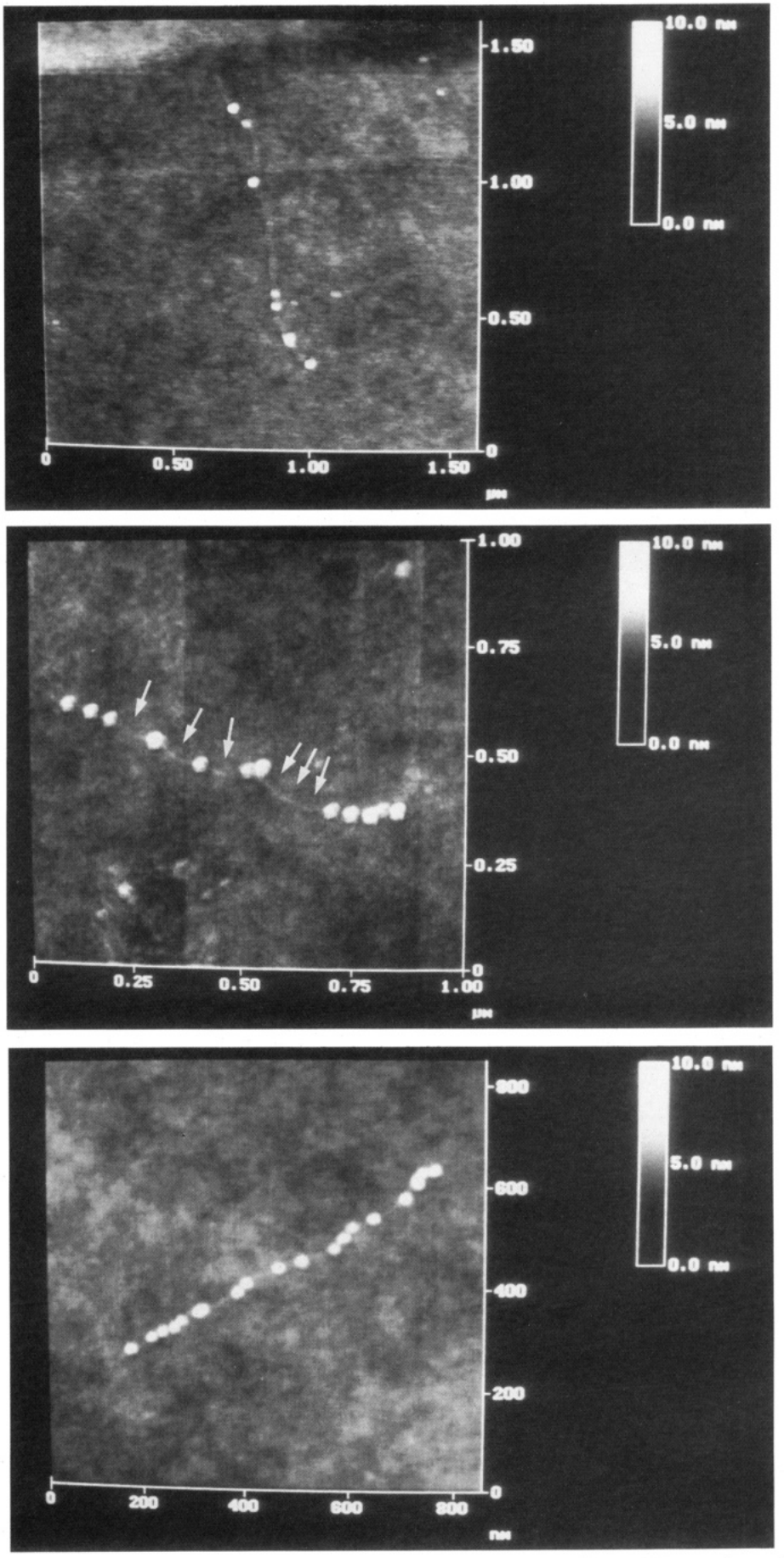

FIGURE 2: (A–C, top to bottom) High-resolution AFM images of three linear 208–18 chromatin fibers with increasing nucleosome core loading: (A) 7, (B) 12, and (C) 18 cores. The chromatin fiber contour lengths were (A) 1164 nm, (B) 852 nm, and (C) 693 nm. The arrows in (B) point to the six unfilled nucleosome positions. Images were obtained using carbonized Si_3N_4 probes.

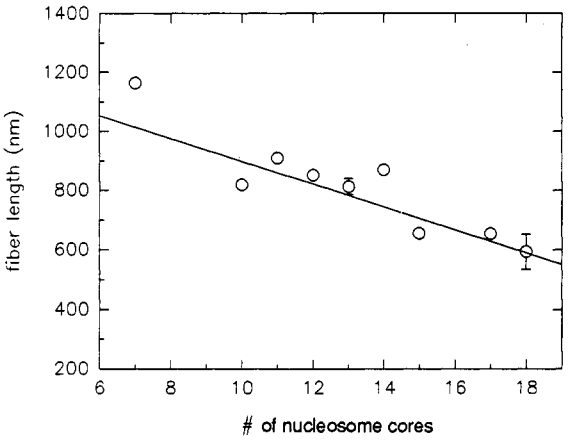

FIGURE 3: Effect of histone octamer loading on chromatin fiber contour length, as determined by AFM. Circles represent AFM measurements showing the compaction of the linear 208–18 DNA sequence induced by increasing levels of histone octamer loading. The solid line represents the expected compaction of the 208–18 DNA sequence (3780 bp) induced by the packaging of 146-bp DNA into nucleosome cores.

or are "shoulder to shoulder"), we measure a center-to-center intercore spacing of 37.2 nm ($n = 36 \pm 8.8$ nm). This value is close to the 32.1-nm intercore spacing expected if all of the directly adjacent cores were precisely positioned on the DNA construct used in this study (i.e., spaced every 208 bp). The accuracy of such center-to-center measurements is limited mainly by the AFM piezo-electric scanner usually calibrated to the atomic spacings of graphite and mica. Consequently, AFM studies involving the effects of various proteins and their modifications (e.g., histone acetylation) on intercore spacing, using reconstituted or native chromatin samples, can be conducted with detection limits on the subnanometer scale. Similar analyses can be performed on any reasonably rigid biological structure exhibiting unique topographies and spacings. Presumably other important DNA binding proteins, such as RNA polymerase II or transcription factors bound to DNA or to nucleosome fibers, can also be imaged on the cover glass with the AFM.

AFM Images of the Closed Circular Chromatin. Scans of these preparations gave AFM images very different from those of linear chromatin. As expected for circular chromatin, the chromatin fibers exhibited a highly tangled, twisted appearance (Figure 4). Despite the tangled appearance of the chromatin fibers, nucleosome cores were detected (Figure 4B). However, since the fibers were highly contorted and did not lie flat on the cover glass, length and core-spacing measurements could not be performed accurately. Relaxation of these samples using a topoisomerase enzyme should allow better imaging of the circular chromatin fibers in the future. Interestingly, only the samples containing extensively cross-linked histone octamers could be imaged reproducibly by AFM. Either the control or un-cross-linked samples did not adhere to the cover glass or the force load of the scanning AFM probe caused destabilization of the nucleosome cores. At this point it appears that glutaraldehyde fixation of the chromatin or extensive cross-linking of the histone octamers is required to obtain good AFM images of the chromatin fibers. Further, chemical fixation may prove useful as a general preparative procedure for samples otherwise unstable under AFM imaging conditions.

DISCUSSION

Some of the nucleosome cores measured by AFM exhibited thicknesses within a few angstroms of the neutron scatter and X-ray diffraction values of 5.5–6.0 nm (Imai et al., 1986; Richmond et al., 1984). However, some cores gave thicknesses of 4.5 nm and as little as 2.5 nm in z-height. It is difficult to determine whether these measurements reflect the true thicknesses of partially hydrated cores or of partially formed cores or if some of the cores were depressed by the force load of the AFM probe (typically 10^{-7}–10^{-8} N in air). Theoretical calculations have predicted that imaging forces exceeding 10^{-11} N should be destructive to biological molecules (Persson, 1987). However, nothing to our knowledge is known about the compressibility or stability of the nucleosome core under AFM imaging conditions. Similar to several AFM reports of naked DNA imaged on mica in air and under fluid (Bustamante et al., 1992; Lyubchenko et al., 1993a; Shaiu et al., 1993), our measurements of the linker DNA in AFM images of chromatin fibers range from only a few angstroms up to 10 Å in z-height above the cover glass. In addition, the apparent z-heights would often vary along the length of individual DNA strands. At certain points along its path, the DNA was obscured by local surface roughness of the cover glass (which exhibited peak-to-valley roughnesses of up to 10 Å), making it nearly indistinguishable from the surrounding substrate. However, in contrast to these reports, Hansma et al. (1993) have observed that the apparent z-height of DNA in AFM images is dependent on the level of DNA hydration, and 2.5-nm z-heights were observed in aqueous media. Although we have not yet obtained AFM images of nucleosome cores in aqueous environments, it will be informative to compare the z-heights of nucleosome cores measured in aqueous fluid with those obtained in air or in propanol. High pressures exerted by the AFM probe during scanning (e.g., $\approx 10^5$ atm in air for a surface area interaction of 1 nm^2), structural collapse of DNA on its binding to the substrate, probe–sample adhesion (Lyubchenko et al., 1993a), and/or influence of the probe's chemical composition (Lyubchenko et al., 1993a) may also explain the numerous reports that apparent z-height measurements are less than the diameter of the DNA. If they occured, local deformations of the DNA and nucleosome core structure by the scanning AFM imaging probe would likely cause a delocalization of probe–sample contact and a loss of resolution. This might explain why angstrom-level AFM images of the exposed top face of the nucleosome core (which should be highly resolvable since it is flat) or of any biomolecular structure remain, thus far, elusive.

Whereas nucleosome core widths measured by AFM typically ranged between 30 and 40 nm, the smallest cores were 27 nm. The thickness and width measurements strongly suggest that the disc-shaped cores, 11 nm in diameter by 5.7 nm in thickness, are positioned lengthwise or "face down" on the glass to maximize surface area interactions. Because the dimensions of the core particle have been accurately determined by neutron scattering and X-ray diffraction (Imai et al., 1986; Richmond et al., 1984), we can with reasonable certainty deconvolve the AFM imaging probe's radius of curvature. Given core dimensions of a 5.7 by 11.0 nm disc, the radius of curvature of the sharpest AFM probes used to image the cores is calculated to be approximately 8.5 nm. This value is consistent with SEM measurements of probe sharpness obtained using the same type of AFM probe (Wolter, 1989) and represents more than 2-fold improvement over the previous generation of commercially available AFM probes (Allen et al., 1992). The carbonized and etched silicone probes used in this study exhibited similar levels of sharpness, although Hansma et al. (1992b) have generated even sharper electron

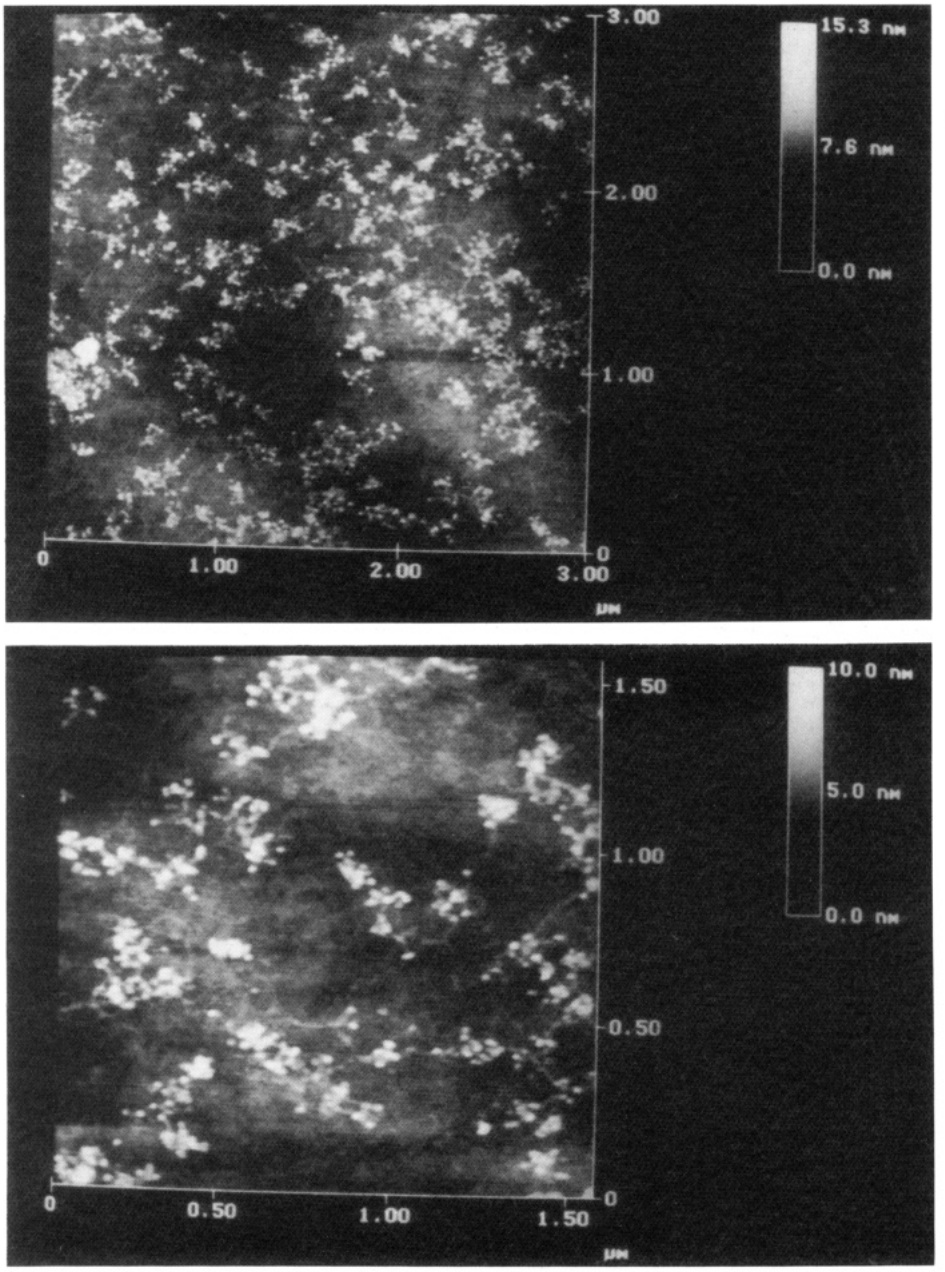

FIGURE 4: (A and B, top to bottom) AFM images showing the highly tangled and beaded appearance of circular chromatin fibers reconstituted using closed circular DNA and cross-linked histone octamers.

beam deposited probes using an ion-milling process. Interestingly, the clearest images of the chromatin fibers were attained using the carbonized probes.

These images of chromatin fibers demonstrate that AFM can provide useful high-resolution structural information of a protein–DNA complex (e.g., internucleosome core spacings and the level of DNA compaction within the cores). Further, AFM is now emerging as a useful structural approach to study the higher order packaging of DNA in chromatin. In some cases AFM provides more clearly resolved images of the chromatin fibers than attained using EM. In addition, chromatin sample preparations for AFM are quick and simple and do not require staining or metal coating. Although superior AFM images of naked DNA fibers can be achieved using mica substrates (M. Allen, unpublished results), we report that cover glass makes a good substrate and high-resolution chromatin fiber AFM images can be obtained.

It appears that even higher resolution AFM imaging of the molecular substructures of the nucleosome will only be achieved if sharper AFM imaging probes (including probe asperities or "nanotips") can be generated and used reliably and/or optimal imaging conditions (including the complex influences of probe–sample forces) are defined more clearly. AFM imaging in fluid environments (Allen et al., 1991; Hansma et al., 1992a; Lyubchenko et al., 1993b) or under high vacuum to reduce the capillary forces that exist in air, the use of compatible probe and substrate materials (Lyubchenko, 1993a; Yang et al., 1992), sample preparations producing more tightly bound specimens (Yang et al., 1992), or noncontact AFM imaging (Wiegrabe et al., 1991) using sharper probes may help to maintain highly localized probe–sample interactions during imaging. One of the AFM probes used in this study appeared to detect a segment of the DNA as it coiled around the central histone octamer (data not shown). However, we do not expect reproducibility of such encouraging images to improve much without distinct improvements in the materials and/or methods used currently. Meanwhile, many new structural biology applications above

the level of atomic structure are now accessible to AFM and more will follow as this technology advances.

ACKNOWLEDGMENT

We gratefully acknowledge Dr. Carlos Bustamante for providing the carbonized AFM probes, Dr. John Breneman for the chicken erythrocyte octamers, and Dr. Nicholas Hud, Joe Lee, Dr. Wigbert Siekhaus, and Michael Wilson for valuable discussions.

REFERENCES

Allen, M. J., Hud, N., Lee, C., Pogany, G., Siekhaus, W. J., & Balhorn, R. (1991) *J. Cell Biol. 115*, 50a.

Allen, M. J., Hud, N., Balooch, M., Tench, R., Siekhaus, W., & Balhorn, R. (1992) *Ultramicroscopy 42–44*, 1095–1100.

Binnig, G., Quate, C. F., & Gerber, Ch. (1986) *Phys. Rev. Lett. 56*, 930–933.

Bustamante, C., Vesenka, J., Tang, C. L., Rees, W., Guthold, M., & Keller, R. (1992) *Biochemistry 31*, 22–26.

Butt, H.-J., Downing, K. H., & Hansma, P. K. (1990) *Biophys. J. 58*, 1473–1480.

Da Silva, L. B., Trebes, J. E., Balhorn, R., Mrowka, S., Anderson, E., Attwood, D. T., Barbee, T. W., Jr., Brase, J., Corzett, M., Gray, J., Koch, J. A., Lee, C., Kern, D., London, R. A., MacGowan, B. J., Matthews, D. L., & Stone, G. (1992) *Science 258*, 269–271.

De Grooth, B. G., & Putman, A. J. (1992) *J. Microsc. 168*, 239–247.

Engel, A. (1991) *Annu. Rev. Biophys. Biophys. Chem. 20*, 79–108.

Germond, J.-E., Bellard, M., Oudet, P., & Chambon, P. (1976) *Nucleic Acids Res. 3*, 3173–3192.

Haberle, W., Horber, J. K. H., & Binnig, G. (1991) *J. Vac. Sci. Technol. B9*, 1210–1213.

Hansma, H. G., Sinsheimer, R. L., Li, M.-Q., & Hansma, P. K. (1992a) *Nucleic Acids Res. 20*, 3585–3590.

Hansma, H. G., Vesenka, J., Siergerist, C., Kelderman, G., Morrett, H., Sinsheimer, R. L., Elings, V., Bustamante, C., & Hansma, P. K. (1992b) *Science 256*, 1180–1184.

Hansma, H. G., Bezanilla, M., Zenhausern, F., Adrian, M., & Sinsheimer, R. L. (1993) *Nucleic Acids Res. 21*, 505–512.

Hansma, P. K., Elings, V. B., Marti, O., & Bracker, C. E. (1988) *Science 242*, 209–216.

Heinzelmann, H., Meyer, E., Rudin, H., & Guntherodt, H. J. (1990) in *Scanning Tunneling Microscopy and Related Methods* (Behm, R. J., Ed.) pp 443–467, Kluwer Academic, Boston.

Henderson, E., Haydon, P. G., & Sakaguchi, D. S. (1992) *Science 257*, 1944.

Hoh, J. H., & Hansma, P. K. (1992) *Trends Cell Biol. 2*, 208–213.

Imai, B. S., Yau, P., Baldwin, J. P., Ibel, K., May, R. P., & Bradbury, E. M. (1986) *J. Biol. Chem. 261*, 8784–8792.

Lyubchenko, Y., Oden, P. I., Lampner, D., Lindsay, S. M., & Dunker, K. A. (1993a) *Nucleic Acids Res. 21*, 1117–1123.

Lyubchenko, Y., Shlyakhtenko, L., Harrington, R., Oden, P., & Lindsay, S. (1993b) *Proc. Natl. Acad. Sci. U.S.A. 90*, 2137–2140.

Norton, V. G., Imai, B. S., Yau, P., & Bradbury, E. M. (1989) *Cell 57*, 449–457.

O'Neill, T. E., Roberge, M., & Bradbury, E. M. (1992) *J. Mol. Biol. 223*, 67–78.

O'Neill, T. E., Smith, J. G., & Bradbury, E. M. (1993) *Proc. Natl. Acad. Sci. U.S.A.* (in press).

Persson, B. N. J. (1987) *Chem. Phys. Lett. 141*, 366–368.

Richmond, T. G., Finch, J. T., Ruchton, B., Rhodes, D., & Klug, A. (1984) *Nature 311*, 532–537.

Shaiu, W.-L., Larson, D. D., Vesenka, J., & Henderson, E. (1993) *Nucleic Acids Res. 21*, 99–103.

Simpson, R. T., Thoma, F., & Brubaker, J. M. (1985) *Cell 42*, 799–808.

Singh, S., & Keller, D. J. (1991) *Biophys. J. 60*, 1401–1410.

Stein, A., Bina-Stein, M., & Simpson, R. T. (1977) *Proc. Natl. Acad. Sci. U.S.A. 74*, 2780–2784.

Vesenka, J., Guthold, M., Tang, C. L., Keller, D., Delaine, E., & Bustamante, C. (1992a) *Ultramicroscopy 42–44*, 1243–1249.

Vesenka, J., Hansma, H., Siegerist, C., Siligardi, G., Schabtach, E., & Bustamante, C. (1992b) *SPIE Proc. 1639*, 127–137.

Wiegrabe, W., Nonnenmacher, M., Guckenberger, R., & Wolter, O. J. (1991) *Microscopy 163*, 79–84.

Wolter, O. (1989) Seminar of the IBM Europe Institute, Garmisch Partenkirchen, Germany, Aug 14–18.

Yang, J., Takeyasu, K., & Shao, Z. (1992) *FEBS Lett. 301*, 173–176.